Am J Physiol Renal Physiol 285: F191–F198, 2003.
First published April 8, 2003; 10.1152/ajprenal.00042.2003.

Injury of the renal microvascular endothelium alters barrier function after ischemia

Timothy A. Sutton,[1] Henry E. Mang,[1] Silvia B. Campos,[1] Ruben M. Sandoval,[1,2] Mervin C. Yoder,[3] and Bruce A. Molitoris[1,2]

[1]*Division of Nephrology, Department of Medicine, Indiana Center for Biological Microscopy, and* [3]*Division of Neonatology, Department of Pediatrics, Indiana University School of Medicine, and* [2]*Roudebush Veterans Affairs Medical Center, Indianapolis, Indiana 46202*

Submitted 3 February 2003; accepted in final form 28 March 2003

Sutton, Timothy A., Henry E. Mang, Silvia B. Campos, Ruben M. Sandoval, Mervin C. Yoder, and Bruce A. Molitoris. Injury of the renal microvascular endothelium alters barrier function after ischemia. *Am J Physiol Renal Physiol* 285: F191–F198, 2003. First published April 8, 2003; 10.1152/ajprenal.00042.2003.—The role of renal microvascular endothelial cell injury in the pathophysiology of ischemic acute renal failure (ARF) remains largely unknown. No consistent morphological alterations have been ascribed to the endothelium of the renal microvasculature as a result of ischemia-reperfusion injury. Therefore, the purpose of this study was to examine biochemical markers of endothelial injury and morphological changes in the renal microvascular endothelium in a rodent model of ischemic ARF. Circulating von Willebrand factor (vWF) was measured as a marker of endothelial injury. Twenty-four hours after ischemia, circulating vWF peaked at 124% over baseline values ($P = 0.001$). The FVB-TIE2/GFP mouse was utilized to localize morphological changes in the renal microvascular endothelium. Immediately after ischemia, there was a marked increase in F-actin aggregates in the basal and basolateral aspect of renal microvascular endothelial cells in the corticomedullary junction. After 24 h of reperfusion, the pattern of F-actin staining was more similar to that observed under physiological conditions. In addition, alterations in the integrity of the adherens junctions of the renal microvasculature, as demonstrated by loss of localization in vascular endothelial cadherin immunostaining, were observed after 24 h of reperfusion. This observation temporally correlated with the greatest extent of permeability defect in the renal microvasculature as identified using fluorescent dextrans and two-photon intravital imaging. Taken together, these findings indicate that renal vascular endothelial injury occurs in ischemic ARF and may play an important role in the pathophysiology of ischemic ARF.

von Willebrand factor; vascular endothelial cadherin; vascular permeability

BOTH SUBLETHAL AND LETHAL tubular epithelial cell injury have been of central importance in explaining the decrement in glomerular filtration rate that is the hallmark of acute renal failure (ARF). However, over the last decade the paradigm of the pathophysiology of ischemic ARF has evolved to include a complex interplay between tubular injury, inflammation, and altered renal hemodynamics. Recent studies have provided further evidence for the role that vascular injury, in particular endothelial cell injury, plays in the pathophysiology of ischemic ARF (5, 46). Endothelial cell swelling, altered endothelial cell-cell attachment, and altered endothelial cell-basement membrane attachment are some of the morphologic alterations that have been observed in the renal microvasculature (5, 12) as well as the cerebral and coronary vasculature (40, 42) after ischemic injury. Functional consequences of these morphological alterations include altered vascular reactivity, increased leukocyte adherence and extravasation, altered coagulation due to loss of normal endothelial function and/or barrier, and increased interstitial edema that have been documented as a consequence of ischemic ARF in animal models (16).

Specialized cellular junctions similar to those in epithelial cells maintain endothelial cell-cell contacts. Tight junctions are more prominent in "tight" vascular beds, such as those between the endothelial cells of the cerebral vasculature forming the blood-brain barrier, whereas they are sparse and simplified in "leaky" vascular beds, such as postcapillary venules (43). Cadherin-containing adherens junctions are ubiquitous between endothelial cells throughout the vasculature (43). Recent studies highlighting the differences in the molecular composition of junctional complexes in various vascular beds, including those within the kidney, provide insight into the potential functional differences in the cellular junctions in these vascular beds (3, 11, 25, 32). Disruption of endothelial adherens junctions in vivo by the use of an inhibitory antibody to vascular endothelial cadherin (VE-cadherin) has been demonstrated to induce gaps between endothelial cells, increase endothelial permeability, and promote the accumulation of inflammatory cells in coronary and pulmonary vascular beds (8). Furthermore, there is evidence from in vitro studies that the interaction of endothelial cell-cell junctions with the actin cytoskeleton plays an important role in regulating endothelial paracellular

Address for reprint requests and other correspondence: T. A. Sutton, Div. of Nephrology/Dept. of Medicine, 1120 South Dr., Fesler Hall 115, Indianapolis, IN 46202 (E-mail: tsutton2@iupui.edu).

The costs of publication of this article were defrayed in part by the payment of page charges. The article must therefore be hereby marked "*advertisement*" in accordance with 18 U.S.C. Section 1734 solely to indicate this fact.

Downloaded from http://ajprenal.physiology.org/ by 10.220.33.6 on January 13, 2017

transport (34). Although the above findings underscore the importance of endothelial cell-cell junctions in maintaining the integrity of the endothelial permeability barrier, there is essentially no in vivo information on the effect of ischemic injury on the function and organization of these intercellular junctions in the renal microvasculature due to previous technical difficulty in visualizing the endothelium of the renal microvasculature in animals and human biopsy samples. However, there are data indicating microvascular congestion and localized interstitial edema after renal ischemia (15, 16). Therefore, we hypothesized that ischemic injury to the kidney results in alterations of the endothelial actin cytoskeleton and endothelial cell-cell junctions that contribute to increased vascular permeability and local interstitial edema. In this study, we demonstrate that ischemic renal injury results in disorganization of the actin cytoskeleton and loss of VE-cadherin localization in the endothelium of the renal microvasculature and that these alterations are accompanied temporally by increased permeability of the renal microvasculature.

MATERIALS AND METHODS

Reagents and antibodies. Rhodamine-conjugated dextran (3,000 mol wt), FITC-conjugated dextran (500,000 mol wt), rhodamine-conjugated-phalloidin, and Hoechst 33342 were from Molecular Probes (Eugene, OR). Rat polyclonal antibodies to mouse VE-cadherin were from BD Pharmingen (San Diego, CA). Affinity-purified Texas red-labeled sheep anti-rat IgG antibodies were from Jackson ImmunoResearch Laboratories (West Grove, PA). An Asserachrom vWF ELISA kit was from Diagnostica Stago (Parsippany, NJ), and a Quantikine M rat IL-6 immunoassay kit was from R&D Systems (Minneapolis, MN).

Animals. Male Sprague-Dawley rats (Harlan, Indianapolis, IN) and male FVB-TIE2/GFP mice, which express green fluorescent protein (GFP) under the direction of the endothelial-specific receptor tyrosine kinase (*Tie2*) promoter (33), were used as described below.

Surgical procedure to induce renal ischemia. All experiments were conducted in accordance with the *Guide for the Care and Use of Laboratory Animals* (Washington, DC: National Academy Press, 1996) and approved by the Institutional Animal Care and Use Committee. Male Sprague-Dawley rats weighing 200–250 g were anesthetized with an intraperitoneal injection of pentobarbital sodium (65 mg/kg) and placed on a homeothermic table to maintain core body temperature at 37°C. For experiments involving measurement of biochemical markers of endothelial injury, a midline incision was made, the renal pedicles were isolated, and bilateral renal ischemia was induced by clamping the renal pedicles for 45 min as previously described (31). Sham surgery consisted of an identical procedure with the exception of immediate release of the microaneurysm clamps. Tail-vein blood samples from experimental, sham, and nonoperative control rats were collected, stored, and processed as per instructions of the Asserachrom vWF ELISA kit. For experiments involving live two-photon microscopic imaging of rat kidneys, a flank incision was made over the left kidney, the renal pedicle was isolated, and unilateral renal ischemia was induced by clamping the left renal pedicle for 45 min as previously described (9). For experiments involving renal ischemia in FVB-TIE2/GFP mice, 20- to 25-g mice were anesthetized utilizing 5% halothane for induction and 1.5% for maintenance and placed on a homeothermic table to maintain core body temperature at 37°C. A midline incision was made, and the left renal pedicle was isolated. Renal ischemia was induced by clamping the renal pedicle for 32 min as described by Kelly et al. (20).

Fluorescence microscopy. Kidney sections from anesthetized mice were fixed ex vivo in 4% paraformaldehyde, and 50-μm vibratome sections were obtained. Sections were stained with rhodamine-phalloidin or rat polyclonal anti-mouse VE-cadherin and polyclonal Texas red-labeled sheep anti-rat IgG secondary antibodies. Images of the microvasculature in the corticomedullary region of the kidney were collected with an LSM-510 Zeiss confocal microscope (Heidelberg, Germany) equipped with argon and helium/neon lasers. For intravital fluorescence microscopy, 100 μl of rhodamine-conjugated dextran (3,000 mol wt, 20 mg/ml in 0.9% saline), 500 μl of FITC-conjugated dextran (500,000 mol wt, 7.5 mg/ml in 0.9% saline), and 400 μl of Hoechst 33342 (1.5 mg/ml in 0.9% saline) were injected via the tail vein into anesthetized rats just before imaging. The left kidney of the anesthetized rat was imaged through a retroperitoneal window via a left-flank incision using a Bio-Rad MRC-1024MP Laser Scanning Confocal/Multiphoton scanner (Hercules, CA) with an excitation wavelength of 800 nm attached to a Nikon Diaphot inverted microscope (Fryer, Huntley, IL) as described by Dunn et al. (9). Image processing was performed utilizing Metamorph software (Universal Imaging, West Chester, PA).

Statistics. Results are expressed as means ± SE and were analyzed for significance by paired and unpaired Student's *t*-tests and ANOVA.

RESULTS

Biochemical evidence of renal endothelial injury during ischemia. A variety of studies have utilized an elevated circulating von Willebrand factor Ag (vWF) concentration as a marker of endothelial cell injury in other organs in response to a variety of insults (1, 6, 13, 19, 28, 35, 37) including ischemia-reperfusion injury to the intestines (1). Therefore, we quantified circulating vWF in Sprageu-Dawley rats as a marker of renal endothelial injury after renal ischemia. Twenty-four hours after a 45-min bilateral renal artery clamp, circulating vWF reached its maximum level and was significantly elevated (Table 1) over baseline preclamp values ($P = 0.001$) and over levels in sham-operated control animals ($P = 0.029$). Circulating vWF levels in sham-operated animals were not significantly different from baseline values at 24 h. Circulating vWF de-

Table 1. *Serum von Willebrand factor increases after renal ischemia*

Time, h	Sham-Operated	Ischemic
24	33.8 ± 16.2	123.9 ± 22.2*†
48	58.0 ± 33.7	85.6 ± 42.7‡

Values are as mean percentages above baseline ± SE. Time is expressed as hours after release of bilateral renal artery clamps. *$P = 0.029$ vs. sham-operated animals. †$P = 0.001$ vs. baseline values. ‡Not significant vs. sham-operated animals.

Downloaded from http://ajprenal.physiology.org/ by 10.220.33.6 on January 13, 2017

creased by 48 h after ischemia and was not significantly elevated over baseline values or over the level in sham-operated control animals.

The actin cytoskeleton of renal microvascular endothelium was disrupted after ischemia. To determine the effect of ischemia on the actin cytoskeleton of the renal microvascular endothelium, sections of normal and ischemic kidneys from FVB-TIE2/GFP mice were stained with rhodamine-phalloidin and examined by confocal microscopy. Under physiological conditions, F-actin staining was predominantly observed along the basal aspect of renal microvascular endothelial cells (Fig. 1*A*). Immediately after 32 min of renal ischemia, alterations in the actin cytoskeleton of the renal microvascular endothelium included F-actin aggregation along the lateral aspects of the cells and increased F-actin aggregation along the basal aspects of the cells (Fig. 1*B*). After 24 h of reperfusion subsequent to ischemia, the F-actin staining pattern more closely resembled the pattern observed under physiological conditions (Fig. 1*C*), although there remained a more aggregated appearance of the F-actin along the basal aspects of the renal microvascular endothelial cells than what was observed under physiological conditions.

Adherens junctions of renal microvascular endothelium were disrupted after ischemia. To determine the effect of ischemia on the adherens junctions of the renal microvascular endothelium, the pattern of VE-cadherin immunostaining was examined by confocal microscopy in sections of normal and ischemic kidneys from FVB-TIE2/GFP mice. Under physiological conditions, VE-cadherin immunostaining was continuous along the renal microvascular endothelium (Fig. 2). Whereas VE-cadherin immunostaining was not limited to intracellular endothelial contacts, it was similar to in vivo VE-cadherin immunostaining observed in other studies (4, 8). After 32 min of ischemia, VE-cadherin staining remained in the renal microvasculature. Twenty-four hours after ischemia, the majority of the renal microvasculature did not stain for VE-cadherin. The loss of VE-cadherin staining after ischemia suggested a disruption of the normal junctional complex between endothelial cells of the renal microvasculature. Seventy-two hours after ischemia, VE-cadherin staining in the renal microvasculature was similar to that observed under physiological conditions.

Alteration in renal microvascular permeability after ischemia. Having demonstrated morphological alterations in the actin cytoskeleton and the adherens junctions of the renal microvascular endothelium after ischemia, we undertook the next study to examine the functional correlate of the observed morphological alterations. Technical considerations limited the effectiveness of two-photon intravital imaging of the corticomedullary region in rodents, as well as intravital imaging of kidneys in FVB-TIE2/GFP mice. Consequently, intravital imaging was performed in the cortical region of rats. To examine alterations in vascular permeability, a rhodamine-conjugated, low-molecular-weight (3,000) neutral dextran and a FITC-conjugated, high-molecular-weight (500,000) neutral dextran were intravenously coinjected into rats under physiological conditions and after ischemia. Injections of fluorescent dextrans were undertaken at selected time points to

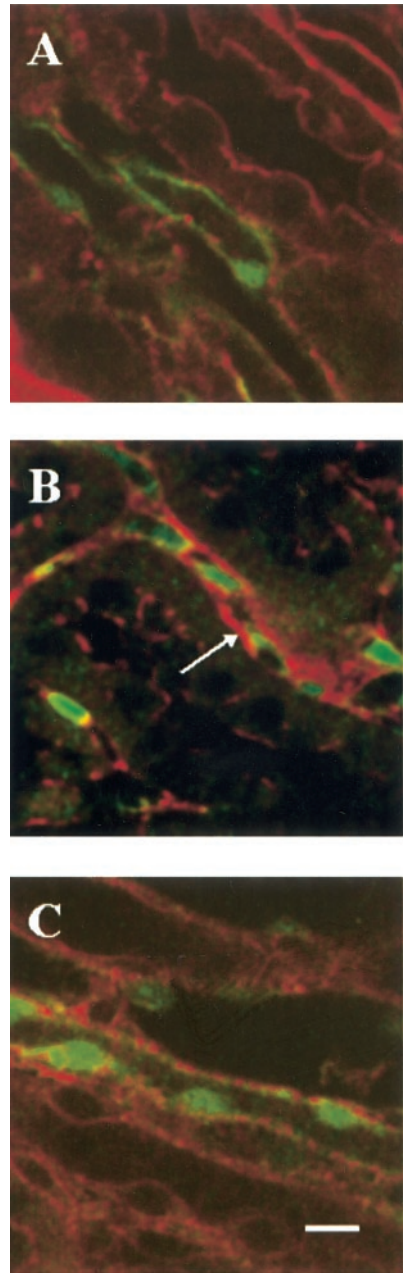

Fig. 1. The actin cytoskeleton of renal endothelial cells is disrupted after renal ischemia. The FVB-TIE2/GFP mouse, which expresses green fluorescent protein (GFP) driven by the endothelial TIE2 promoter, was utilized to localize changes in the actin cytoskeleton of the microvascular endothelium (green) in the corticomedullary region of the kidney. Rhodamine-phalloidin was used to stain F-actin (red). *A*: nonischemic kidney. *B*: kidney after 32 min of renal artery clamping. Note the increase in F-actin polymerization and aggregation in endothelial cells of the renal microvasculature (arrow). *C*: kidney after 24 h of reperfusion following 32 min of renal artery clamping. Bar = 10 μm.

Downloaded from http://ajprenal.physiology.org/ by 10.220.33.6 on January 13, 2017

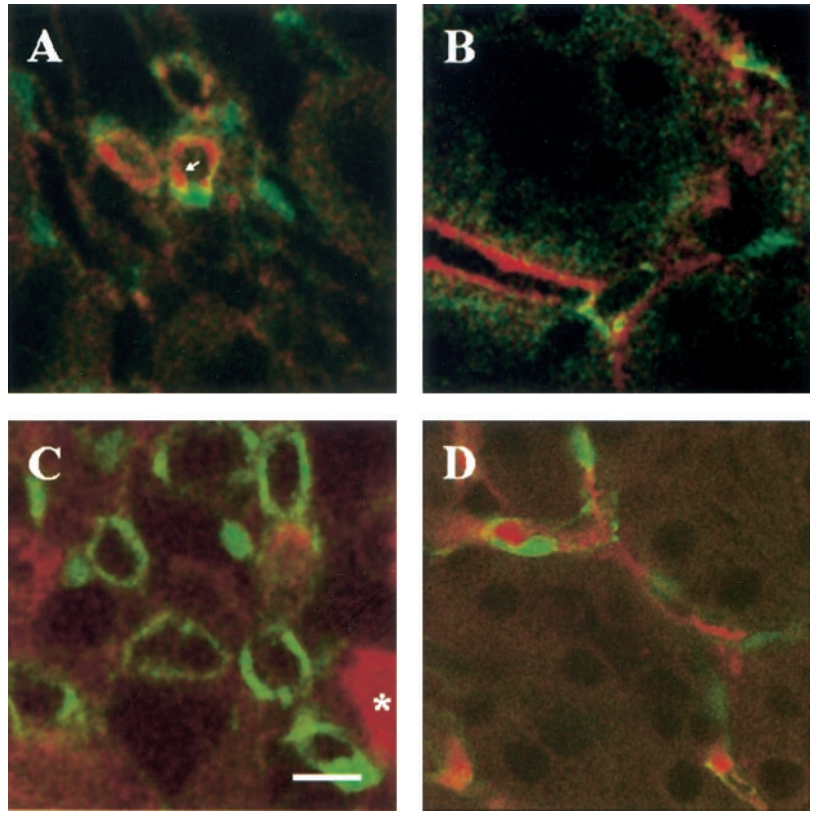

Fig. 2. Adherens junctions of renal microvascular endothelium were disrupted after ischemia. The FVB-TIE2/GFP mouse was utilized to localize changes in vascular endothelial (VE)-cadherin (red) staining of the microvascular endothelium (green) in the corticomedullary region of the kidney after ischemia. While VE-cadherin staining was present under physiological conditions (arrow in *A*) and immediately after 32 min of ischemia (*B*), loss of VE-cadherin staining was noted after 24 h of reperfusion following 32 min of ischemia (*C*). Of note, immunostaining was observed in the lumens (*) of tubules at 24 h postischemia; however, this pattern of staining was seen in the secondary antibody controls (data not shown), suggesting that the staining in the tubular lumen was nonspecific secondary antibody staining and not VE-cadherin staining. Seventy-two hours after 32 min of ischemia, VE-cadherin staining was similar to that under physiological conditions. Bar = 10 μm.

evaluate the microvascular permeability at that particular point in time. The renal microcirculation was observed in vivo utilizing dual-photon confocal microscopy. Injection of the fluorescent-labeled dextrans under physiological conditions revealed that the high-molecular-weight dextran was maintained in the vascular space and was not filtered by the glomerulus, whereas, the low-molecular-weight dextran was rapidly filtered into the tubules, accumulated in endosomes of the proximal tubule, and concentrated in the lumen of the distal tubules as previously described (9) (Fig. 3*A*). Areas of diminished microvascular blood flow were observed immediately after renal ischemia; however, occasional areas of leakage of either the low- or high-molecular-weight dextran from the microvascular space into the renal interstitium were not observed until 2 h after renal ischemia (arrows, Fig. 3*B*). Leakage of both dextrans appeared to reach its greatest extent 24 h after ischemia (Fig. 3*C*). Forty-eight hours after ischemia, there were still some patchy areas of leakage but the extent of the permeability defect appeared to have improved significantly (Fig. 3*D*). Glomerular filtration of the high-molecular-weight dextran into the tubular lumen was not observed after ischemia at any of the time points studied. As might be anticipated, leakage of the smaller dextran into the interstitium was more diffuse than that of the larger dextran (Fig. 4). Interestingly, areas where leakage of both dextrans occurred were more often observed in areas of markedly diminished microvascular flow (a supplementary video of Fig. 4*C* can be viewed at http://ajprenal.physiology.org/cgi/content/full/00042.2003/DC1).

DISCUSSION

Endothelial dysfunction and vasomotor alterations of the renal vasculature have played a conceptual role in the pathophysiology of ARF for a number of years (12). However, recent work by Brodsky et al. (5), in particular, has brought to light the vulnerability of the renal microvascular endothelium to ischemic injury and has highlighted the renal vascular endothelium as a potential target for injury in renal ischemia. To further an understanding of the role endothelial cell injury plays in ischemic ARF, we have utilized a renal artery clamp model of ischemic ARF in rats and mice. While this model is imperfect, it has provided valuable insight into the pathophysiology of ischemic injury to the kidney (27). Our study has served to extend confirmed previous findings and to begin to examine some of the mechanisms by which renal microvascular endothelial injury may contribute to altered function in one of the myriad roles to which the endothelium is subservient.

Our finding of an elevation in circulating vWF after renal ischemic injury contributes to the evidence that the renal vascular endothelium is injured. In other organ systems, release of vWF from the endothelium has been demonstrated to occur in a biphasic fashion in

Downloaded from http://ajprenal.physiology.org/ by 10.220.33.6 on January 13, 2017

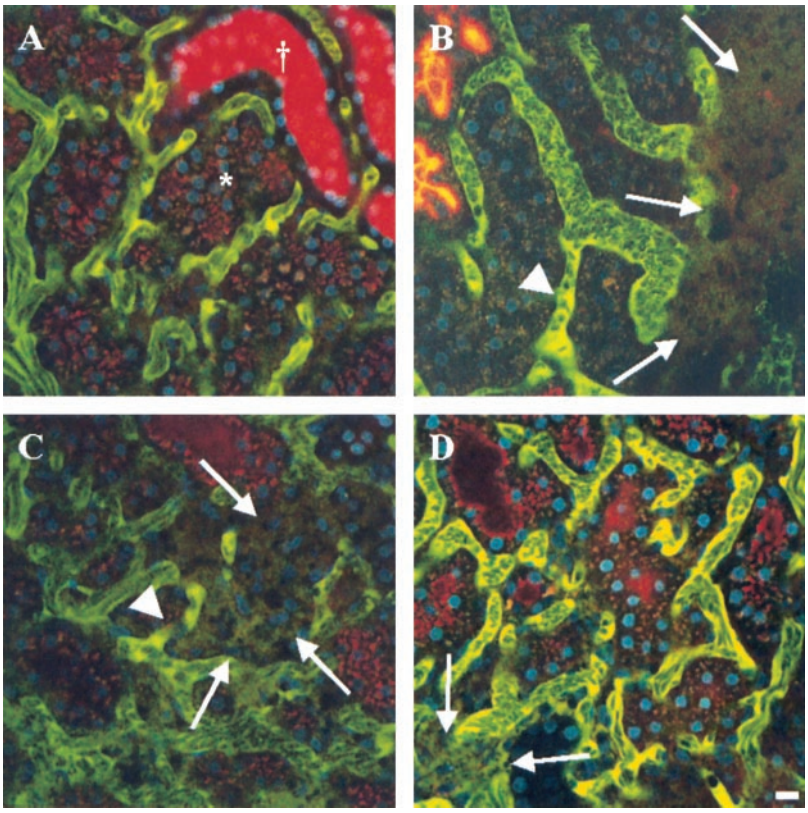

Fig. 3. Ischemia results in altered renal vascular permeability. A 500,000-mol wt, FITC-labeled dextran (green), 3,000-mol wt, rhodamine-labeled dextran (red), and the nuclear stain Hoechst 33342 (blue) were injected via the tail vein into sham-operated, nonischemic rats (*A*) and into rats after 2 (*B*), 24 (*C*), and 48 (*D*) h of reperfusion following 45 min of ischemia. Intravital images of the kidneys were obtained via a retroperitoneal approach. The large FITC-labeled dextran was generally retained in the vascular space and identifies the microvasculature. Signal voids in the vascular space are due to the relative rapid movement of cellular elements (red and white blood cells) compared with the speed of image acquisition. Proximal tubules are identified by the red punctate appearance from the internalization of the small rhodamine-labeled dextran (*). Distal tubules are identified by the luminal concentration of the small rhodamine-labeled dextran (†). Note the close approximation of the tubules and microvasculature in the sham-operated control rat (*A*). Scattered areas of extravasation of both the small and large dextrans (arrows) from the vascular space into the interstitium were noted as early as 2 h after reperfusion (*B*). The extent of extravasation peaked at ~24 h of reperfusion (*C*) and returned to close to normal after 48 h of reperfusion (*D*). Note the areas of diminished blood flow (large arrowheads in *B* and *C*) identified by intravascular cellular elements that appear stationary during the time frame of image acquisition. Bar = 10 μm.

response to ischemia-reperfusion injury (10, 39). These studies suggest that hypoxia, as well as reperfusion, mediate endothelial release of vWF via potentially different mechanisms. Furthermore, inflammatory processes can contribute to endothelial vWF release (41). The peak elevation of circulating vWF in our study was monophasic and occurred 24 h after the initial ischemic insult; thus continued hypoxia, reperfusion injury, and/or inflammatory processes could separately or collectively play a role in endothelial release of vWF in the renal artery-clamp model of ischemic ARF. Whereas the peak increase in vWF occurred at the same time as the peak in serum creatinine in our study, given the large molecular weight of the various circulating forms of vWF (500–20,000), it is doubtful that reduced renal clearance of vWF significantly contributed to the elevation in circulating vWF. While the intent of this portion of the investigation was to simply provide evidence for endothelial injury, the utility of such a finding may ultimately lie in the ability to characterize the nature and extent of the underlying injury by circulating markers of endothelial injury and thus provide a useful clinical correlate for disease severity, prognosis, and therapeutic intervention. For example, endothelial release of IL-6 has been demonstrated to be of prognostic value in sepsis where endothelial injury plays an important role in the underlying pathophysiology (14). Although a previous study of intestinal ischemia-reperfusion injury did not demonstrate a correlation between histological injury scores and the level of circulating vWF (1), the pattern of circulating vWF multimers or the pattern of vWF coupled with other markers of injury may in the end prove to be a useful clinical tool in renal ischemia-reperfusion injury.

Our examination of the morphological alterations in renal microvascular endothelial cells revealed that the normal structure of the actin cytoskeleton in renal microvascular endothelial cells is disrupted after ischemia. Alteration of the normal actin cytoskeleton of endothelial cells in vitro has been demonstrated with ATP depletion as a model of ischemic injury and with H_2O_2 as a model of oxidant-mediated reperfusion injury. ATP depletion has been demonstrated to rapidly and reversibly disrupt the normal cortical and basal F-actin structures in endothelial cells (17, 24, 45), resulting in F-actin aggregation and polymerization. Oxidant-mediated endothelial cell injury also has been demonstrated to disrupt the cortical actin band in cultured endothelial cells (18, 29, 47). We observed that disruption of the actin cytoskeleton in endothelial cells of the renal microvasculature subjected to ischemic injury in vivo was most prominent immediately after the ischemic insult. Consistent with the above-mentioned in vitro findings, we observed an alteration of the normal cortical and basal F-actin structures of the endothelial cell with an apparent increase in F-actin polymerization and aggregation at the basal and basolateral aspects of endothelial cells after ischemia. This F-actin polymerization and aggregation was reminiscent of the alterations observed after ischemia in proximal tubular epithelial cells (30) and renal vascular smooth muscle cells (26). Of note, the TIE2 promoter

Downloaded from http://ajprenal.physiology.org/ by 10.220.33.6 on January 13, 2017

has been reported to be upregulated in vitro by hypoxia in human umbilical vascular endothelial cells (7). In our in vivo study, we did not observe a difference in the number of vessels or a change in the intensity of GFP signal at the selected time points.

The alterations in the actin cytoskeleton of renal microvascular endothelial cells preceded alterations in VE-cadherin staining at endothelial cell-cell junctions. These findings are consistent with a mechanism by which loss of integrity of the actin cytoskeleton contributes to breakdown of the actin-associated adherens junctions and contributes to the concomitant permeability defect. Much of the present knowledge regarding the mechanisms regulating endothelial cell-cell interaction during ischemic and oxidant injury has come from in vitro models utilizing cultured endothelial cells. ATP depletion of endothelial cell monolayers and exposure of endothelial monolayers to oxidants such H_2O_2 have both been demonstrated to increase endothelial permeability and intercellular gap formation (22, 36, 38). Increased endothelial permeability in these models has been associated with internalization of VE-cadherin from endothelial adherens junctions (2, 21). Although we did not observe internalization of VE-cadherin after ischemia in vivo, other mechanisms including cleavage of VE-cadherin as described in a previous in vivo study (4) may account for the diminished VE-cadherin staining observed in our study.

The utilization of two-photon intravital microscopy to visualize the permeability defect in the renal microvasculature after ischemia is a particular strength of our study. The power of this imaging technique is demonstrated in our ability not only to simultaneously evaluate the disparity in the permeability defect of two differently sized fluorescent probes but also to observe a correlation, in a timed-image series, between alterations in blood flow and severity of the permeability defect. These data imply continued reduced blood flow results in increased permeability defects between endothelial cells. Although these observations were limited to the cortical area of rats due to technical considerations, presumably the permeability defect in the corticomedullary area would be even more pronounced than what we observed in the cortical microvasculature (16). Implications for leakage of plasma from the vascular space and increased interstitial edema, especially in the corticomedullary area, include further diminishment of the compromised medullary blood flow by extrinsic compression of peritubular capillaries (23) and by hemoconcentration as observed in other organs (44).

In summary, we have demonstrated that renal microvascular injury manifested by disruption of the actin cytoskeleton and adherens junction of endothelial cells occurs after ischemic injury and that this injury is probably fundamental to increased microvascular per-

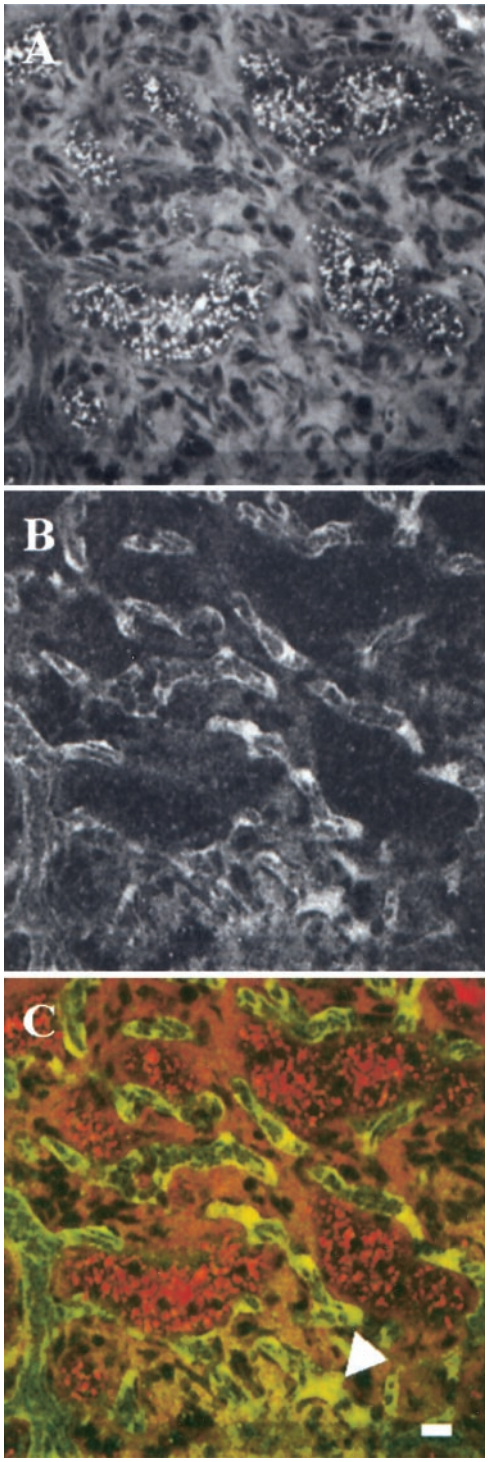

Fig. 4. Extent of microvascular permeability defect is heterogeneous. A 3,000-mol wt, rhodamine-labeled dextran (*A*; red in *C*) and a 500,000-mol wt, FITC-labeled dextran (*B*; green in *C*) were injected via the tail vein into a rat after 24 h of reperfusion following 45 min of ischemia. *A*–*C* are images obtained from the same field. *A*: demonstration of the extent of microvascular extravasation of the low-molecular-weight dextran. *B*: demonstration of the extent of microvascular extravasation of the high-molecular-weight dextran. *C*: color overlay of *A* and *B*, with the low-molecular-weight dextran in red, the high-molecular-weight dextran in green, and the arrowhead indicating an area of diminished microvascular flow. Bar = 10 μm. A supplementary video of *C* is a time series taken from the same field as shown and is composed of a 30-frame series of images collected at 2 frames/s, projected at 10 frames/s, demonstrating the diminished flow in the area of the greatest permeability defect.

Downloaded from http://ajprenal.physiology.org/ by 10.220.33.6 on January 13, 2017

meability and renal interstitial edema. Further characterization of the implications of renal microvascular injury may provide new diagnostic and therapeutic avenues in ischemic ARF.

We acknowledge Simon Atkinson, Ken Dunn, and Katherine Kelly for valuable discussions.

DISCLOSURES

This work was supported by National Institutes of Health (NIH) Grant DK-60621–61594, the Ralph W. and Grace M. Showalter Research Trust, and National Kidney Foundation of Indiana grants (to T. A. Sutton), NIH Grant HL-63169 (to M. C. Yoder), and NIH Grants DK-41126, DK-53465, and DK-61594, and Veterans Affairs Medical Research Service grants (to B. A. Molitoris).

REFERENCES

1. **Abu-Zidan FM, Winterbourn CC, Bonham MJ, Simovic MO, Buss H, and Windsor JA.** Small bowel ischaemia-reperfusion increases plasma concentrations of oxidised proteins in rats. *Eur J Surg* 165: 383–389, 1999.
2. **Alexander JS, Jackson SA, Chaney E, Kevil CG, and Haselton FR.** The role of cadherin endocytosis in endothelial barrier regulation: involvement of protein kinase C and actin-cadherin interactions. *Inflammation* 22: 419–433, 1998.
3. **Aurrand-Lions M, Johnson-Leger C, Wong C, Du Pasquier L, and Imhof BA.** Heterogeneity of endothelial junctions is reflected by differential expression and specific subcellular localization of the three JAM family members. *Blood* 98: 3699–3707, 2001.
4. **Bianchi C, Araujo EG, Sato K, and Sellke FW.** Biochemical and structural evidence for pig myocardium adherens junction disruption by cardiopulmonary bypass. *Circulation* 104: I319–324, 2001.
5. **Brodsky SV, Yamamoto T, Tada T, Kim B, Chen J, Kajiya F, and Goligorsky MS.** Endothelial dysfunction in ischemic acute renal failure: rescue by transplanted endothelial cells. *Am J Physiol Renal Physiol* 282: F1140–F1149, 2002.
6. **Chaloner C, Blann A, and Braganza JM.** Endothelial cell harbingers of adult respiratory distress syndrome in acute pancreatitis (Abstract). *Lancet* 344: 1167, 1994.
7. **Christensen RA, Fujikawa K, Madore R, Oettgen P, and Varticovski L.** NERF2, a member of the Ets family of transcription factors, is increased in response to hypoxia and angiopoietin-1: a potential mechanism for Tie2 regulation during hypoxia. *J Cell Biochem* 85: 505–515, 2002.
8. **Corada M, Mariotti M, Thurston G, Smith K, Kunkel R, Brockhaus M, Lampugnani MG, Martin-Padura I, Stoppacciaro A, Ruco L, McDonald DM, Ward PA, and Dejana E.** Vascular endothelial-cadherin is an important determinant of microvascular integrity in vivo. *Proc Natl Acad Sci USA* 96: 9815–9820, 1999.
9. **Dunn KW, Sandoval RM, Kelly KJ, Dagher PC, Tanner GA, Atkinson SJ, Bacallao RL, and Molitoris BA.** Functional studies of the kidney of living animals using multicolor two-photon microscopy. *Am J Physiol Cell Physiol* 283: C905–C916, 2002.
10. **Farrell AJ, Williams RB, Stevens CR, Lawrie AS, Cox NL, and Blake DR.** Exercise induced release of von Willebrand factor: evidence for hypoxic reperfusion microvascular injury in rheumatoid arthritis. *Ann Rheum Dis* 51: 1117–1122, 1992.
11. **Fina L, Molgaard HV, Robertson D, Bradley NJ, Monaghan P, Delia D, Sutherland DR, Baker MA, and Greaves MF.** Expression of the CD34 gene in vascular endothelial cells. *Blood* 75: 2417–2426, 1990.
12. **Flores J, DiBona DR, Beck CH, and Leaf A.** The role of cell swelling in ischemic renal damage and the protective effect of hypertonic solute. *J Clin Invest* 51: 118–126, 1972.
13. **Gralnick HR, McKeown LP, Wilson OM, Williams SB, and Elin RJ.** Von Willebrand factor release induced by endotoxin. *J Lab Clin Med* 113: 118–122, 1989.
14. **Hack CE and Zeerleder S.** The endothelium in sepsis: source of and a target for inflammation. *Crit Care Med* 29: S21–S27, 2001.
15. **Hellberg PO, Bayati A, Kallskog O, and Wolgast M.** Red cell trapping after ischemia and long-term kidney damage. Influence of hematocrit. *Kidney Int* 37: 1240–1247, 1990.
16. **Hellberg PO, Kallskog OT, Ojteg G, and Wolgast M.** Peritubular capillary permeability and intravascular RBC aggregation after ischemia: effects of neutrophils. *Am J Physiol Renal Fluid Electrolyte Physiol* 258: F1018–F1025, 1990.
17. **Hinshaw DB, Armstrong BC, Beals TF, and Hyslop PA.** A cellular model of endothelial cell ischemia. *J Surg Res* 44: 527–537, 1988.
18. **Hinshaw DB, Burger JM, Armstrong BC, and Hyslop PA.** Mechanism of endothelial cell shape change in oxidant injury. *J Surg Res* 46: 339–349, 1989.
19. **Jones DK, Perry EM, Grosso MA, and Voelkel NF.** Release of von Willebrand factor antigen (vWF:Ag) and eicosanoids during acute injury to the isolated rat lung. *Am Rev Respir Dis* 145: 1410–1415, 1992.
20. **Kelly KJ, Williams WW Jr, Colvin RB, Meehan SM, Springer TA, Gutierrez-Ramos JC, and Bonventre JV.** Intercellular adhesion molecule-1-deficient mice are protected against ischemic renal injury. *J Clin Invest* 97: 1056–1063, 1996.
21. **Kevil CG, Ohno N, Gute DC, Okayama N, Robinson SA, Chaney E, and Alexander JS.** Role of cadherin internalization in hydrogen peroxide-mediated endothelial permeability. *Free Radic Biol Med* 24: 1015–1022, 1998.
22. **Kevil CG, Oshima T, Alexander B, Coe LL, and Alexander JS.** H_2O_2-mediated permeability: role of MAPK and occludin. *Am J Physiol Cell Physiol* 279: C21–C30, 2000.
23. **Klingebiel T, von Gise H, and Bohle A.** Morphometric studies on acute renal failure in humans during the oligoanuric and polyuric phases. *Clin Nephrol* 20: 1–10, 1983.
24. **Kuhne W, Besselmann M, Noll T, Muhs A, Watanabe H, and Piper HM.** Disintegration of cytoskeletal structure of actin filaments in energy-depleted endothelial cells. *Am J Physiol Heart Circ Physiol* 264: H1599–H1608, 1993.
25. **Kurihara H, Anderson JM, and Farquhar MG.** Diversity among tight junctions in rat kidney: glomerular slit diaphragms and endothelial junctions express only one isoform of the tight junction protein ZO-1. *Proc Natl Acad Sci USA* 89: 7075–7079, 1992.
26. **Kwon O, Phillips CL, and Molitoris BA.** Ischemia induces alterations in actin filaments in renal vascular smooth muscle cells. *Am J Physiol Renal Physiol* 282: F1012–F1019, 2002.
27. **Lieberthal W and Nigam SK.** Acute renal failure. II. Experimental models of acute renal failure: imperfect but indispensable. *Am J Physiol Renal Physiol* 278: F1–F12, 2000.
28. **Lip GY and Blann A.** Von Willebrand factor: a marker of endothelial dysfunction in vascular disorders? *Cardiovasc Res* 34: 255–265, 1997.
29. **Lum H, Barr DA, Shaffer JR, Gordon RJ, Ezrin AM, and Malik AB.** Reoxygenation of endothelial cells increases permeability by oxidant-dependent mechanisms. *Circ Res* 70: 991–998, 1992.
30. **Molitoris BA, Geerdes A, and McIntosh JR.** Dissociation and redistribution of Na^+,K^+-ATPase from its surface membrane actin cytoskeletal complex during cellular ATP depletion. *J Clin Invest* 88: 462–469, 1991.
31. **Molitoris BA, Wilson PD, Schrier RW, and Simon FR.** Ischemia induces partial loss of surface membrane polarity and accumulation of putative calcium ionophores. *J Clin Invest* 76: 2097–2105, 1985.
32. **Morita K, Sasaki H, Furuse M, and Tsukita S.** Endothelial claudin: claudin-5/TMVCF constitutes tight junction strands in endothelial cells. *J Cell Biol* 147: 185–194, 1999.
33. **Motoike T, Loughna S, Perens E, Roman BL, Liao W, Chau TC, Richardson CD, Kawate T, Kuno J, Weinstein BM, Stainier DY, and Sato TN.** Universal GFP reporter for the study of vascular development. *Genesis* 28: 75–81, 2000.
34. **Navarro P, Caveda L, Breviario F, Mandoteanu I, Lampugnani MG, and Dejana E.** Catenin-dependent and -indepen-

Downloaded from http://ajprenal.physiology.org/ by 10.220.33.6 on January 13, 2017

dent functions of vascular endothelial cadherin. *J Biol Chem* 270: 30965–30972, 1995.
35. **Newsholme SJ, Thudium DT, Gossett KA, Watson ES, and Schwartz LW.** Evaluation of plasma von Willebrand factor as a biomarker for acute arterial damage in rats. *Toxicol Pathol* 28: 688–693, 2000.
36. **Noll T, Muhs A, Besselmann M, Watanabe H, and Piper HM.** Initiation of hyperpermeability in energy-depleted coronary endothelial monolayers. *Am J Physiol Heart Circ Physiol* 268: H1462–H1470, 1995.
37. **Novotny MJ, Turrentine MA, Johnson GS, and Adams HR.** Experimental endotoxemia increases plasma von Willebrand factor antigen concentrations in dogs with and without free-radical scavenger therapy. *Circ Shock* 23: 205–213, 1987.
38. **Ochoa L, Waypa G, Mahoney JR Jr, Rodriguez L, and Minnear FL.** Contrasting effects of hypochlorous acid and hydrogen peroxide on endothelial permeability: prevention with cAMP drugs. *Am J Respir Crit Care Med* 156: 1247–1255, 1997.
39. **Pinsky DJ, Naka Y, Liao H, Oz MC, Wagner DD, Mayadas TN, Johnson RC, Hynes RO, Heath M, Lawson CA, and Stern DM.** Hypoxia-induced exocytosis of endothelial cell Weibel-Palade bodies. A mechanism for rapid neutrophil recruitment after cardiac preservation. *J Clin Invest* 97: 493–500, 1996.
40. **Pomfy M and Huska J.** The state of the microcirculatory bed after total ischaemia of the brain. An experimental ultrastructural study. *Funct Dev Morphol* 2: 253–258, 1992.
41. **Reinhart K, Bayer O, Brunkhorst F, and Meisner M.** Markers of endothelial damage in organ dysfunction and sepsis. *Crit Care Med* 30: S302–S312, 2002.
42. **VanBenthuysen KM, McMurtry IF, and Horwitz LD.** Reperfusion after acute coronary occlusion in dogs impairs endothelium-dependent relaxation to acetylcholine and augments contractile reactivity in vitro. *J Clin Invest* 79: 265–274, 1987.
43. **Vestweber D.** Molecular mechanisms that control endothelial cell contacts. *J Pathol* 190: 281–291, 2000.
44. **Vollmar B, Glasz J, Leiderer R, Post S, and Menger MD.** Hepatic microcirculatory perfusion failure is a determinant of liver dysfunction in warm ischemia-reperfusion. *Am J Pathol* 145: 1421–1431, 1994.
45. **Watanabe H, Kuhne W, Spahr R, Schwartz P, and Piper HM.** Macromolecule permeability of coronary and aortic endothelial monolayers under energy depletion. *Am J Physiol Heart Circ Physiol* 260: H1344–H1352, 1991.
46. **Yamamoto T, Tada T, Brodsky SV, Tanaka H, Noiri E, Kajiya F, and Goligorsky MS.** Intravital videomicroscopy of peritubular capillaries in renal ischemia. *Am J Physiol Renal Physiol* 282: F1150–F1155, 2002.
47. **Zhao Y and Davis HW.** Hydrogen peroxide-induced cytoskeletal rearrangement in cultured pulmonary endothelial cells. *J Cell Physiol* 174: 370–379, 1998.

Downloaded from http://ajprenal.physiology.org/ by 10.220.33.6 on January 13, 2017